### Title

The oncogenic fusion protein EML4-NTRK3 requires three salt bridges for stability and biological activity.




### Journal

Vaccine Reports, 10(16)

### ISSN

2405-8440



### Authors

Jiang, Zian

Meyer, April

Yang, Wei

et al.



### Publication Date

2024-08-30

### DOI

10.1016/j.heliyon.2024.e36278

Heliyon 10 (2024) e36278

Contents lists available at ScienceDirect

Heliyon

journal homepage: www.cell.com/heliyon

Research article

# The oncogenic fusion protein EML4-NTRK3 requires three salt bridges for stability and biological activity

Zian Jiang [a], April N. Meyer [a], Wei Yang [a], Daniel J. Donoghue [a,b,*]

[a] Department of Chemistry and Biochemistry, University of California San Diego, La Jolla, CA, 92093-0367 USA
[b] UCSD Moores Cancer Center, University of California San Diego, La Jolla, CA, 92093-0367, USA

ARTICLE INFO

*Keywords:*
Oncogenic fusion protein
Infantile fibrosarcoma
Congenital mesoblastic nephroma
Soft tissue sarcoma
Coiled coil

ABSTRACT

*Aim of study:* Chromosomal translocations involving neurotrophic receptor tyrosine kinases (NTRKs) have been identified in 20 % of soft tissue sarcomas. This work focuses on the EML4-NTRK3 translocation identified in cases of Infantile Fibrosarcoma, which contains the coiled-coil multimerization domain of Echinoderm Microtubule-like protein 4 (EML4) fused with the tyrosine kinase domain of Neurotrophic Receptor Tyrosine Kinase 3 (NTRK3). The aim of the study was to test the importance of tyrosine kinase activity and multimerization for the oncogenic activity of EML4-NTRK3.

*Methods:* These studies examined EML4-NTRK3 proteins containing a kinase-dead or WT kinase domain, together with mutations in specific salt bridge residues within the coiled-coil domain. Biological activity was assayed using focus assays in NIH3T3 cells. The MAPK/ERK, JAK/STAT3 and PI3K/AKT pathways were analyzed for downstream activation of signaling pathways. Localization of EML4-NTRK3 proteins was examined by immunofluorescence microscopy, and the ability of the EML4 coiled-coil domain to drive protein multimerization was examined by biochemical assays.

*Results:* Activation of EML4-NTRK3 relies on both the tyrosine kinase activity of NTRK3 and salt-bridge stabilization within the coiled-coil domain of EML4. The tyrosine kinase activity of NTRK3 is essential for the biological activation of EML4-NTRK3. Furthermore, EML4-NTRK3 activates downstream signaling pathways MAPK/ERK, JAK/STAT3 and PKC/PLCγ. The disruption of three specific salt bridge interactions within the EML4 coiled-coil domain of EML4-NTRK3 blocks downstream activation, biological activity, and the ability to hetero-multimerize with EML4. We also demonstrate that EML4-NTRK3 is localized in the cytoplasm and fails to associate with microtubules.

*Concluding statement:* These data suggest potential therapeutic strategies for Infantile Fibrosarcoma cases bearing EML4-NTRK3 fusion through inhibition of salt bridge interactions and disruption of multimerization.

## 1. Introduction

Infantile Fibrosarcoma (IFS) is the most common type of non-rhabdomyosarcoma soft tissue tumor which generally occurs in

* Corresponding author. Department of Chemistry and Biochemistry, University of California San Diego, La Jolla, CA, 92093-0367, USA.
*E-mail addresses:* zij005@ucsd.edu (Z. Jiang), ameyer@ucsd.edu (A.N. Meyer), wey069@ucsd.edu (W. Yang), ddonoghue@ucsd.edu (D.J. Donoghue).

https://doi.org/10.1016/j.heliyon.2024.e36278
Received 15 September 2023; Received in revised form 7 August 2024; Accepted 13 August 2024
Available online 13 August 2024

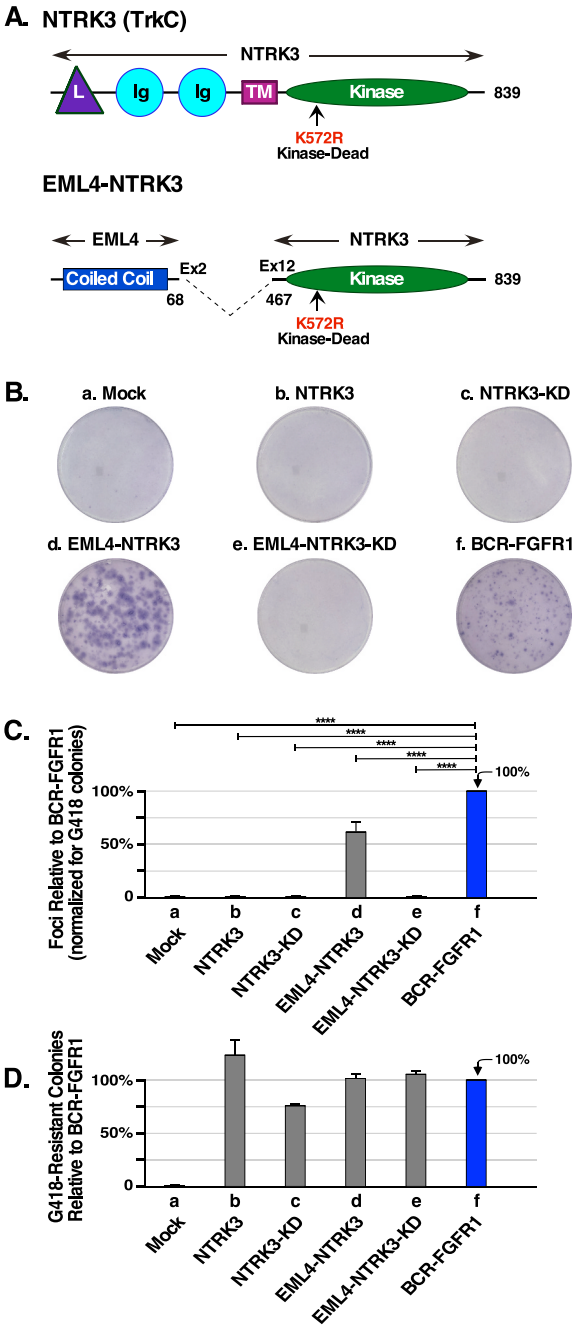


**Fig. 1. Domain organization and cell transformation assays of EML4-NTRK3. (A)** Schematic of NTRK3 and EML4-NTRK3. The K572R kinase dead mutation of NTRK3 is shown. NTRK3 contains a leucine-rich domain (L), an extracellular ligand binding domain containing immunoglobulin-like domains (Ig), a transmembrane domain (TM), and a tyrosine kinase domain (Kinase). The EML4-NTRK3 fusion protein is encoded by EML4 exons 1 and 2, which are fused to exons 12–18 of NTRK3. EML4 contributes a coiled-coil domain of 68 amino acids to the EML4-NTRK3 fusion. **(B)** Plates of NIH3T3 cells demonstrate transformation by EML4-NTRK3 constructs in a focus formation assay. After fixation, plates were stained using Giemsa. The transfected constructs are indicated. **(C)** The graph presents the number of foci after normalization for transfection efficiency, and presented as a percentage relative to BCR-FGFR1, a positive control for foci formation, −/+ standard error of the mean (SEM). Assays were carried out a minimum of three times for every DNA construct. Results of paired two tailed t-tests are shown, where **** indicates significance at $P \leq 0.0001$. **(D)** As a control for equivalent transfection and expression, G418-resistant colonies are shown in comparison with the positive control BCR-FGFR1.

infants and children less than 2 years old. The main course of treatment for IFS is surgical excision, after which there is a low chance of metastasis and a high probability of long-term survival, above 90 % [1,2]. IFS tumors reside in subcutaneous fat, muscle, fascia and tendons [3], and they are morphologically described as spindle-shaped cells in layers of dilated blood vessels arranged in a herringbone pattern [4]. Chromosomal translocations are often identified in IFS, with the oncogenic fusion ETV6-NTRK3 occurring frequently in above 90 % of IFS. ETV6-NTRK3 consists of the helix-loop-helix (HLH) domain of ETV6 (ETS variant transcription factor 6) joined to the protein tyrosine kinase domain of NTRK3 [5–7].

In addition to ETV6-NTRK3, recent studies have identified another recurrent translocation in IFS involving Echinoderm Microtubule-associated protein-Like 4 (EML4) joined to NTRK3 [4,8]. This novel fusion has been found recurrently in children with IFS and also congenital mesoblastic nephroma ranging from the age of 6 days to 1 year old [9] (Fig. 1A). The EML4-NTRK3 fusions consist of exons 1 and 2 of EML4 joined with exons 12–18 of NTRK3, encompassing the coiled-coil domain of EML4 and the tyrosine kinase domain of NTRK3 [4]. The EML4 N-terminal domain has been shown to form a parallel trimeric coiled-coil structure, of which residues 14–44 have been described in a crystal structure [10]. Specific salt bridges have been identified as conserved between EML proteins [10], presumed to stabilize the triple helix, which are retained in the EML4-NTRK3 fusion. Other domains of EML4 which are not included in the EML4-NTRK3 fusion are the "Tandem Atypical Propeller domain" (TAPE domain), which includes the "Hydrophobic Motif in EML Proteins" (HELP motif), WD repeats, and a microtubule binding motif. Prior studies have shown that EML4-NTRK3 promotes anchorage-independent growth of NIH3T3 cells and tumor formation in NOD scid gamma (NSG) mice [4].

A previous study compared the frequencies of ETV6-NTRK3 and EML4-NTRK3 fusions in 63 documented cases of IFS, mammary analog secretory carcinoma, congenital mesoblastic nephroma, and secretory breast sarcoma, which are the common tumor types for ETV6-NTRK3. Of these archival cases, 23 cases were found to bear the ETV6-NTRK3 fusion while EML4-NTRK3 was identified in three cases, two of which were IFS [9]. The fusion partner for both ETV6-NTRK3 and EML4-NTRK3 is NTRK3, or Neurotrophic Receptor Tyrosine Kinase 3, one of a small family of three related receptors including NTRK1 and NTRK2, also known as Tropomyosin-Related Kinases (TrkA, TrkB, and TrkC) [11]. Each NTRK receptor binds with varying affinities to unique ligands inducing cell proliferation and survival. NTRK1/2/3 are often activated by nerve growth factor (NGF), brain-derived neurotrophic factor (BDNF), and neurotrophin-3 (NT-3), respectively, while different receptor-ligand combinations bind with lesser affinity [5,12]. Upon binding of NT-3, NTRK3 can activate various signaling pathways including Ras/MEK/MAPK, PI3K/AKT, JAK2/STAT3 and phospholipase C-gamma (PLCγ) pathways, which can regulate the survival, cell differentiation and apoptosis in neurons [5,11]. Overexpression of NTRK3 occurs in various cancers such as glioma (91.8 %), thyroid cancer (87 %) and breast cancer (82.4 %) [13–15]. Importantly, NTRK3 has been found joined to a diverse array of over 20 fusion partners [5]. As such, NTRK3 fusions including EML4-NTRK3, ETV6-NTRK3, SPECC1L-NTRK3 have been characterized along with several NTRK1 fusions among cases of pediatric STS [5]. Soft tissue sarcomas represent 7 % of cancers in individuals less than 15 years of age; thus, novel fusions present an important area of study for the development of therapeutic targets [16]. Due to alternative splicing, NTRK3 has several isoforms and the isoform frequently found in chromosomal rearrangements has 18 exons, where exons 13–18 encodes the tyrosine kinase domain of NTRK3 [17].

We chose to study EML4-NTRK3 because of the novelty of the trimeric coiled-coil domain – a multimerization domain exhibited by few other fusion proteins. This is in contrast to the SAM-PNT motif (Sterile alpha motif/pointed domain) present in ETV6-NTRK3, which is a much different multimerization motif with the SAM domain organized as a small five-helix bundle which drives dimerization or potentially larger polymeric assemblages [18,19]. The study presented here explores the requirements and mechanisms of activation of EML4-NTRK3 and its effects on signaling pathways that can lead to cell proliferation, differentiation, survival, and adhesion. The EML4-NTRK3 fusion used in this study is essentially identical and has the same coding sequence as all EML4-NTRK3 fusions in clinical samples with EML4 exon 2 fused to NTRK3 exon 12 [9,20–22]. In addition, we explore the importance of salt bridge residues in the trimerization domain of EML4, previously identified in a study of native proteins in the EML family (EML1-4) [10]. Through mutation of the salt bridge residues, we examined whether disruption of the electrostatic interactions of the salt bridges would result in reduced biological activity of the EML4-NTRK3 fusion protein. We show that disruption of the salt bridges leads to a reduction of downstream signaling pathways, reduced biological activity in transformation assays, and reduced multimerization of the fusion protein. We also demonstrate that EML4-NTRK3 localizes diffusely in the cytoplasm, unlike native EML4 which associates with microtubules.

## 2. Materials and methods

### 2.1. DNA constructs

EML4 consists of 981 residues (Uniprot Q9HC35-1) encoded by 24 exons; the EML4 plasmid (pCMV6-Entry-EML4) was obtained from Origene (Watertown, MA, USA). NTRK3 exists as multiple isoforms, depending on splice isoforms and variable noncoding exons [5]. The canonical sequence Uniprot Q16288-1, also referred to as NT-3 growth factor receptor Isoform A, consists of 839 residues (Uniprot Q16288-1) encoded by 18 exons (Ensemble Transcript: ENST00000629765.3). The NTRK3 plasmid (pDONR223-NTRK3) was purchased from Addgene (Watertown, MA, USA). A stop codon (TGA) and an *Xba*I site were added to the 3' end of the NTRK3 coding region by site-directed mutagenesis. Currently, only one EML4-NTRK3 fusion variant has been identified, which joins the end of EML4 exon 2 to the beginning of NTRK3 exon 12 [4,23]. Using restriction sites *Eco*RI and *Xba*I, the genes encoding EML4 and NTRK3 were subcloned into the vector pcDNA3. A *Cla*I site was introduced after residue S68 in EML4 and before amino acid P467 in NTRK3 using PCR site-directed mutagenesis. The internal *Cla*I site and *Xba*I site were used to subclone exons 12–18 of NTRK3 into the EML4 pcDNA3, creating the EML4-NTRK3 fusion. All EML4-NTRK3 genes, whether expressed in pcDNA3 clones or in pLXSN clones, exhibit the identical DNA sequence around the ATG initiation codon. The major difference is the presence of the Human Cytomegalovirus

(CMV) immediate-early promoter allowing high-level expression in pcDNA3 clones [24], versus the Moloney Murine Leukemia Virus (MoMLV) LTR promoter allowing stable long-term expression in pLXSN clones [25].

All the salt bridge point mutations described were created using PCR site-directed mutagenesis. The constructs Flag-NTRK3 and Flag-EML4-NTRK3 were made using PCR site-directed insertions [26]. Using *Eco*RI and *Xba*I, NTRK3 and EML4-NTRK3 constructs were subcloned into the pLXSN vector [25] for NIH3T3 transformation assays. The Flag-EML4 1–68 clone, referred to as cc-EML4, encoding only the N-terminal coiled-coil domain of EML4, was derived from Flag-EML4-NTRK3 using an adapter to introduce a stop codon after residue S68 of EML4, and which also deleted the remainder of EML4-NTRK3.

### 2.2. Antibodies and reagents

Antibodies were obtained as follow: NTRK3 (Abcam EPR17341 ab181560), P-NTRK (Cell Signaling 4621S C50F3), MAPK (Cell Signaling 9102S p44/42 MAPK Erk1/2), P-MAPK (Cell Signaling 4370S P-p44/42 MAPK T202/Y204 D13.14.4E), STAT3 (Cell Signaling 9139S 124H6), P-STAT3 (Cell Signaling 9145S D3A7 Y705), PLCγ (Santa Cruz sc-81), P-PLCγ (Cell Signaling 2821S Y783), Flag M2 (Sigma F3165), Myc (Santa Cruz sc-40 9E10), Myc (Cell Signaling 2276, 9B11), β-tubulin (Santa Cruz sc-9104 H-235). Reagents for Enhanced Chemiluminescence (ECL), including Horseradish peroxidase (HRP) anti-mouse (NA931V) and HRP anti-rabbit (NA934V) were obtained from Cytiva. Reagents for fluorescence microscopy included Alexa Fluor 488 donkey anti-mouse (A21202 Invitrogen), Alexa Fluor 594 goat anti-rabbit (A11012 Invitrogen), Hoescht 33342 (Tocris Bioscience 5117), and Prolong Gold antifade reagent (Invitrogen, Carlsbad, CA, USA). Other reagents included G-418 Sulfate (Fisher Scientific), Lipofectamine 2000 (Invitrogen), and Protein A-Sepharose (Sigma P3391).

### 2.3. Cell transfection, immunoprecipitation, immunoblot analysis

HEK293T cells were grown in 10 % FBS, 1 % Pen/Strep and plated at $1 \times 10^6$ cells per 10 cm plate. Cells were transfected with 2–5 μg of the EML4-NTRK3 pcDNA3 constructs using calcium phosphate transfection at 3 % $CO_2$ for 16 h, moved to 10 % $CO_2$ for 7 h, and starved with FBS-free DMEM for 17 h before harvest [27]. Cells were lysed using RIPA buffer [50 mM Tris HCl pH 8.0, 150 mM NaCl, 1 % Triton X-100, 0.5 % sodium deoxycholate, 0.1 % SDS, 50 mM NaF, 1 mM sodium orthovanadate, 1 mM PMSF and 10 μg/mL aprotinin]. Protein concentrations were quantitated by Lowry Assay and 20–40 μg of protein was loaded on either 10 % or 12.5 % SDS-PAGE gels for immunoblot analysis [27]. After electrophoresis, proteins were transferred to Immobilon-P membrane (Millipore, Burlington, MA, USA). Membranes were blocked in 5 % bovine serum albumin (BSA)/0.1 % Tween 20-TBS or 5 % nonfat milk/0.1 % Tween 20-TBS.

For immunoprecipitation, cells were lysed in E1A Lysis Buffer [250 mM NaCl, 50 mM HEPES, 5 mM EDTA and 0.1 % NP-40, 1 mM sodium orthovanadate, 1 mM PMSF and 10 μg/mL aprotinin] and Lowry assay was used to determine total protein concentration. 300 μg protein was incubated with rocking overnight at 4 °C with primary antibodies before the addition of Protein A-sepharose beads (Sigma P3391). After rocking for 2 h at 4 °C, complexes were washed with E1A wash buffer [125 mM NaCl, 50 mM HEPES, 5 mM EDTA, and 0.2 % NP-40] 5 times for 10 min each. Complexes were disrupted by adding equal volume of 2 × sample buffer and boiling for 5 min and analyzed on 10 % SDS-PAGE.

#### 2.3.1. Focus assay

NIH3T3 cells were seeded at $4 \times 10^5$ cells per 60 mm plate [27]. The cells were transfected with 10 μg of pLXSN plasmid DNA using Lipofectamine 2000 and fed with 10 % CS-DMEM 24 h after transfection [28]. The cells were re-fed with 2.5 % CS-DMEM every 3–4 d before fixation. Cells were fixed with methanol, stained with Geimsa after 14 d and the Geneticin (G418)-resistant colonies were scored to determine the transfection efficiency [27]. Numbers of foci were counted, normalized for transfection efficiency, and then quantitated to determine the standard error of the mean (SEM), relative to a positive control. Images of tissue culture plates showing colony formation were photographed using an iPhone 8 Plus, placed on top of a small illuminated light box with a square hole for the camera aperture.

### 2.4. Immunofluorescence analysis

NIH3T3 cells were transfected using calcium phosphate, as described above, using 10 μg of the pcDNA3-EML4, pcDNA3-Flag-NTRK3 and pcDNA3-Flag-EML4-NTRK3 constructs. Cells were seeded at $1.5 \times 10^5$ cells on 60 mm plates with glass coverslips (Neuvitro, Vancouver, WA, USA). Microtubule co-staining was performed as described [29,30]. Brinkley Buffer 1980 (BRB80), which contains 80 mM PIPES pH6.8, 1 mM $MgCl_2$, 1 mM EGTA, was used to make microtubule stabilizing buffer (MTSB), which contains 1 x BRB and 0.5 M EGTA. Coverslips with cells were extracted for microtubules in 0.5 % Triton X-100/MTSB for 30 s in 37 °C and fixed in ice-cold methanol for 3 min. Coverslips were rehydrated with 0.1 % TBS-T (0.15 M NaCl, 0.02 M Tris-Cl pH 7.4, 0.1 % Triton X-100) three times for 5 min each and blocked in Abdil (0.1 % Triton X-100, 2 % BSA, 0.1 % $NaN_3$). Antibody dilutions were made with Abdil and washes were performed with 0.1 % TBS-T. Coverslips not stained for β-tubulin were fixed with 4 % paraformaldehyde/PBS, then permeabilized with 0.1 % Triton X-100/PBS, and then blocked with 5 % BSA/PBS. Antibody dilutions were made using 5 % BSA/PBS and washes were performed using PBS. Coverslips were mounted using Prolong Gold anti-fade reagent. A Leica SP8 inverted confocal microscope was employed to examine coverslips (UC San Diego Neuroscience Core Facility).

## 3. Results

### 3.1. Biological activity of EML4-NTRK3

We constructed the oncogenic fusion EML4-NTRK3, which retains the N-terminal coiled-coil domain of EML4 joined to the tyrosine kinase domain of NTRK3 (Fig. 1A). A kinase-dead mutation, K572R, was introduced into both NTRK3 and EML4-NTRK3 to determine whether the transforming ability of EML4-NTRK3 depends on the tyrosine kinase activity of NTRK3 (Fig. 1A). These constructs were assayed in a pLXSN vector [25] using NIH3T3 cell transformation assays in comparison with a previously characterized fusion protein BCR-FGFR1 [31] as a positive control. We chose this classic assay due to its historical use for the identification of oncogenes [32–35]. In this assay, the presence of an oncogene allows transfected NIH3T3 cells to escape contact inhibition, resulting in the appearance of visible foci. EML4-NTRK3 formed slightly lower levels of foci compared to BCR-FGFR1 and, interestingly, the foci formed are larger in size compared to BCR-FGFR1 (Fig. 1B). Other constructs, including wild type NTRK3, kinase-dead NTRK3 K572R, and kinase-dead EML4-NTRK3 K572R did not form detectable foci (Fig. 1B). As a result, the transforming ability of EML4-NTRK3 clearly depends on the tyrosine kinase activity of NTRK3. The statistical significance of these results is also presented (Fig. 1C), using two-tailed paired t-tests comparing each clone with BCR-FGFR1.

Using the pLXSN vector [25], each gene is expressed from the retroviral Moloney Murine Leukemia Virus (MoMLV) LTR promoter, allowing long-term expression. In addition, this vector contains the Neo gene, conferring resistance to Geneticin (G418), under control of the SV40 promoter. The transfections are normalized by plating transfected cells in media with the aminoglycoside antibiotic Geneticin. The colonies that form are then counted, allowing each clone's focus-forming ability to be quantitated. This provides a valuable control that each construct is expressed. The G418-resistant colonies for each construct, relative to the positive control BCR-FGFR1, are shown in Fig. 1D.

### 3.2. The short coiled-coil EML4 trimerization domain contains three salt bridges

The coiled-coil domain of EML4, defined by residues 1 to 68, was previously shown to assume a parallel triple helix stabilized by three interhelical salt bridges [10]. These salt bridges maintain the register of the three parallel alpha helices (Fig. 2A) and, as each salt bridge is repeated three-fold, this leads to a total of nine salt bridges stabilizing this structure. The side-view crystal structure of the trimeric coiled coil shows the three salt bridges occurring between Arg23 and Glu28 (#1), Arg30 and Glu35 (#2), and Glu37 and Lys42 (#3) (Fig. 2B). There are 6 heptad repeats in the EML4 coiled-coil domain, in which the heptad positions are conventionally labelled from "a" to "g" [36] (Fig. 2A–C). In a triple helix, charged amino acid side chains in positions "e" and "g" in one alpha helix have the potential to form electrostatic interactions with those in the neighboring alpha helix, stabilizing the structure of the trimeric coiled coil, as shown in Fig. 2C and D.

### 3.3. Disruption of EML4 salt bridges abolishes biological activity and downstream signaling

The coiled-coil domain of EML4 presents a potential therapeutic target as it contributes to the biological activity of EML4-NTRK3, as demonstrated previously in soft agar colony formation assays [4] and in the work presented here. Thus, we explored the importance of salt bridges in the EML4 coiled-coil domain to determine whether they are essential for the oncogenic activation of EML4-NTRK3. The three salt bridges in the parallel coiled-coil domain of EML4, between Arg23 and Glu28 (#1), Arg30 and Glu35 (#2), and Glu37 and Lys42 (#3) were disrupted by mutating one residue of each pair to the opposite charge to abolish the electrostatic interactions. Each of the resulting single mutants, designated #1, #2, or #3, exhibited a drastic decrease in cell transforming ability of approximately 80 % (Fig. 3A and B). When two or three salt bridge mutations were combined (#1+#2, #2+#3, #1+#3, #1+#2+#3), all biological activity as measured by NIH3T3 transformation assays was lost (Fig. 3A and B). The statistical significance of these results is also presented (Fig. 3A), using two-tailed paired t-tests comparing each clone with EML4-NTRK3.

Since the salt bridge residues are essential for the cell transforming ability, we examined their effects on phosphorylation of the NTRK3 tyrosine kinase domain, and on signaling pathways including MAPK, STAT3, and PLCγ1 in HEK293T cells (Fig. 3C). Interestingly, phosphorylation of the NTRK3 tyrosine kinase domain for the fusions containing the single and double salt bridge mutants was similar to that of EML4-NTRK3 (Fig. 3C, top panel, Lanes 2–8). However, phosphorylation of the NTRK3 tyrosine kinase domain was almost completely abolished by the triple salt bridge mutant (Fig. 3C, top panel, Lane 9). The antisera used to detect P-NTRK3 detects phosphorylation of Tyr709/710 of NTRK3, which are two of the major phosphorylation sites within the activation loop. Activation loop phosphorylation is thought to be one of the earliest steps in RTK activation, bringing about a major conformational change in the kinase domain which potentiates additional phosphorylation events and the recruitment of signaling molecules. Tyrosine phosphorylation of these activation loop tyrosine residues promotes activation and precedes phosphorylation of other tyrosine residues in NTRK3, which are required for full activation [5,37,38]. The observation that the double mutants shown in Fig. 3B significantly attenuate signaling by MAPK, STAT3, and PLCγ1, as well as biological activity (Fig. 3A), whereas the P-NTRK3 signal of these same mutants is largely unchanged, reflects a state of incomplete kinase activation.

Fig. 3D presents quantitation of the signaling pathways examined in Fig. 3C, using three independent datasets. With respect to P-NTRK3, a significant diminution is observed only for one of the double mutants (#1 + 2) and for the triple salt bridge mutant. For the effects of the single salt bridge mutants on P-MAPK, P-STAT3, and P-PLCγ1, with few exceptions (mutant #1 for P-STAT3, mutant #3 for P-PLCγ1), the apparent effects are not significant. However, for each of the double mutants as well as for the triple salt bridge mutant, the effects on P-MAPK, P-STAT3, and P-PLCγ1 are highly significant.

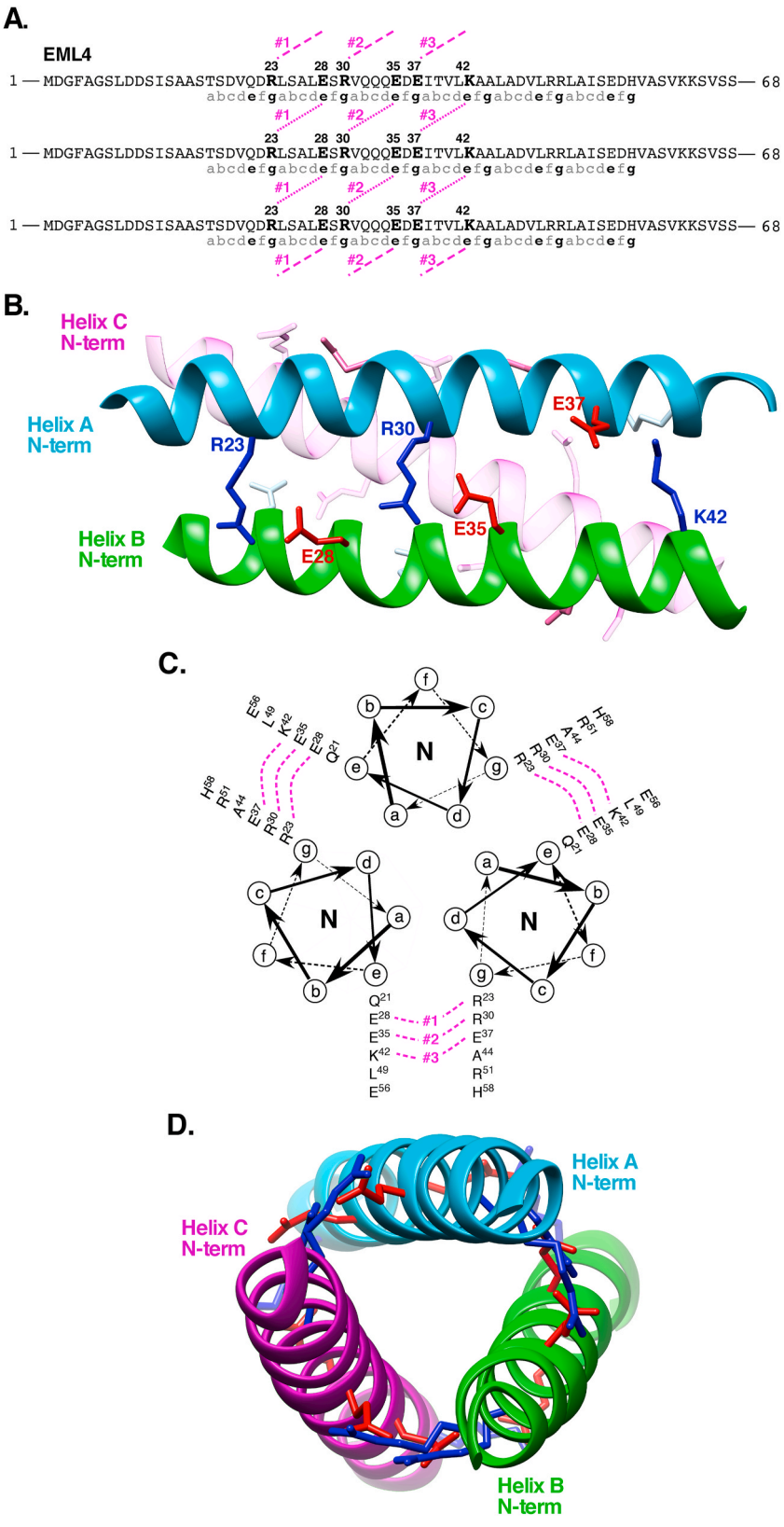


*(caption on next page)*

**Fig. 2. Structure of the parallel triple-stranded coiled-coil domain of EML4 showing the location of three salt bridges. (A)** The amino acid sequence of the N-terminal coiled-coil domain of EML4 is shown, highlighting individual residues that participate in salt bridges in the trimeric coiled coil. The heptad positions are also indicated (a–g). **(B)** The side-view crystal structure of the EML4 trimeric coiled coil domain is shown (PDB code 4CGC), as viewed with Chimera software. Positive residues R23, R30, K42 are in blue, while negative residues E28, E35, E37 are in red. **(C)** The parallel heptad repeats of the trimeric coiled coil domain are shown with the salt bridge residues in the "e" and "g" positions. The interhelical salt bridges are shown between residues R23 and E28 (#1), R30 and E35 (#2), E37 and K42 (#3). **(D)** The top-view crystal structure of the EML4 trimeric coiled-coil domain is presented using Chimera software. Positive residues R23, R30, K42 are in blue while negative residues E28, E35, E37 are in red. (For interpretation of the references to colour in this figure legend, the reader is referred to the Web version of this article.)

In summary, these results suggest a model in which activation of EML4-NTRK3 diminishes progressively with increased disruption of the stabilizing salt bridges, as seen in the NIH3T3 focus formation assays. The residual P-NTRK3 signal for the single and double mutants shows that these mutations lead to autophosphorylation of the activation loop tyrosine residues (Y709/Y710) (Fig. 3C, top panel); however, this may not reflect the totality of tyrosine phosphorylation that occurs in a fully activated EML4-NTRK3 complex in which additional tyrosine phosphorylation may be required for recruiting and activating the downstream signaling proteins MAPK, STAT3 and PLCγ1.

### *3.4. The localization of EML4-NTRK3 is distinct from either parental protein*

We next wished to investigate the cellular localization of EML4-NTRK3 using NIH3T3 cells. EML4 is known to localize in the cytoplasm and associates with microtubules [10], while NTRK3 is a Type I integral membrane protein [39]. Using indirect immunofluorescence, we first confirmed the membrane localization of NTRK3. For this purpose, we inserted a Flag tag at the beginning of the N-terminal extracellular domain of NTRK3, immediately after the signal peptide cleavage site. Without permeabilizing the membrane, indirect immunofluorescent staining was observed only on the periphery of the cell, clearly delineating the plasma membrane (Fig. 4A). However, following membrane permeabilization, staining was observed diffusely throughout the cell (Fig. 4B). We also examined the localization of EML4 by double staining cells for Myc-tagged EML4 and β-tubulin, which confirmed the previously reported microtubule association of EML4 [10] (Fig. 4C–E).

To determine the localization of the fusion protein EML4-NTRK3, permeabilized cells were stained for the FLAG tag, located at the N-terminus of EML4-NTRK3, which showed diffused cytoplasmic staining (Fig. 4F). Double staining of the same cell with antibodies recognizing β-tubulin showed little evidence of colocalization of EML4-NTRK3 with microtubules (Fig. 4G and H). Thus. we conclude that the N-terminal EML4 coiled-coiled domain present in the fusion protein EML4-NTRK3 is not sufficient for microtubule association. The basic region between the coiled-coil and TAPE domains of EML4 has been shown to contribute to the microtubule interaction of EML4 [40]; as this region is absent in the EML4-NTRK3 fusion, this provides a likely explanation for the lack of microtubule binding by EML4-NTRK3.

Given that the EML4-NTRK3 fusion protein loses the N-terminal signal peptide of NTRK3 and, therefore, should lack the ability to undergo membrane insertion, we anticipated that EML4-NTRK3 would exhibit a cytoplasmic localization. This was confirmed by the absence of immunofluorescent staining in non-permeabilized cells using anti-Flag antiserum (Fig. 4I); however, after permeabilization and staining of the same cell with a second antiserum (anti-NTRK3) to detect NTRK3, EML4-NTRK3 was observed to be exclusively cytoplasmic (Fig. 4J and K). Using antiserum to detect the FLAG-tagged EML4 domain of EML4-NTRK3 in permeabilized cells, a similar diffuse staining was observed throughout the cytoplasm (Fig. 4L).

These results demonstrate that EML4-NTRK3 does not undergo microtubule association and presents as a diffusely localized cytoplasmic protein which is largely excluded from the nucleus.

### *3.5. Disruption of three salt bridges abrogates heterodimerization with EML4*

The activation of receptor tyrosine kinase fusion proteins is dependent on the multimerization of the N-terminal fusion partner. We investigated the requirements of multimerization by examining the interaction between the EML4-NTRK3 and EML4. We hypothesized that EML4-NTRK3 might associate with the coiled-coil domain of full-length EML4, and that the salt bridge mutants in the fusion protein would potentially disrupt this association by abrogating the electrostatic interactions between the corresponding alpha helices in the coiled-coil domain.

Given that all the single and double salt bridge mutants exhibited similar effects on cell transformation and downstream activation, we included only EML4(R23E)-NTRK3 and EML4(R23E/R30E)-NTRK3 in subsequent assays, together with the triple mutant EML4 (R23E/R30E/K42E)-NTRK3. HEK293T cells were co-transfected with various EML4-NTRK3 derivatives together with full-length Myc-tagged EML4. Lysates were immunoprecipitated with anti-NTRK3 antiserum, and then immunoblotted with α-c-Myc serum to detect associated EML4 (Fig. 5A, top panel). EML4-NTRK3 and EML4(R23E)-NTRK3 showed strong association with EML4 (Fig. 5A, Lanes 3 and 4). The association was abolished when two or three salt bridges were mutated as in EML4(R23E/R30E)-NTRK3 and EML4 (R23E/R30E/K42E)-NTRK3 (Fig. 5A, Lanes 5 and 6). These data demonstrate that the hetero-oligomerization between EML4-NTRK3 and EML4 requires the salt bridge electrostatic interactions in the coiled-coil domains and that the salt bridge residues function cooperatively to maintain the interactions and the stability of the coiled-coil trimerization domain.

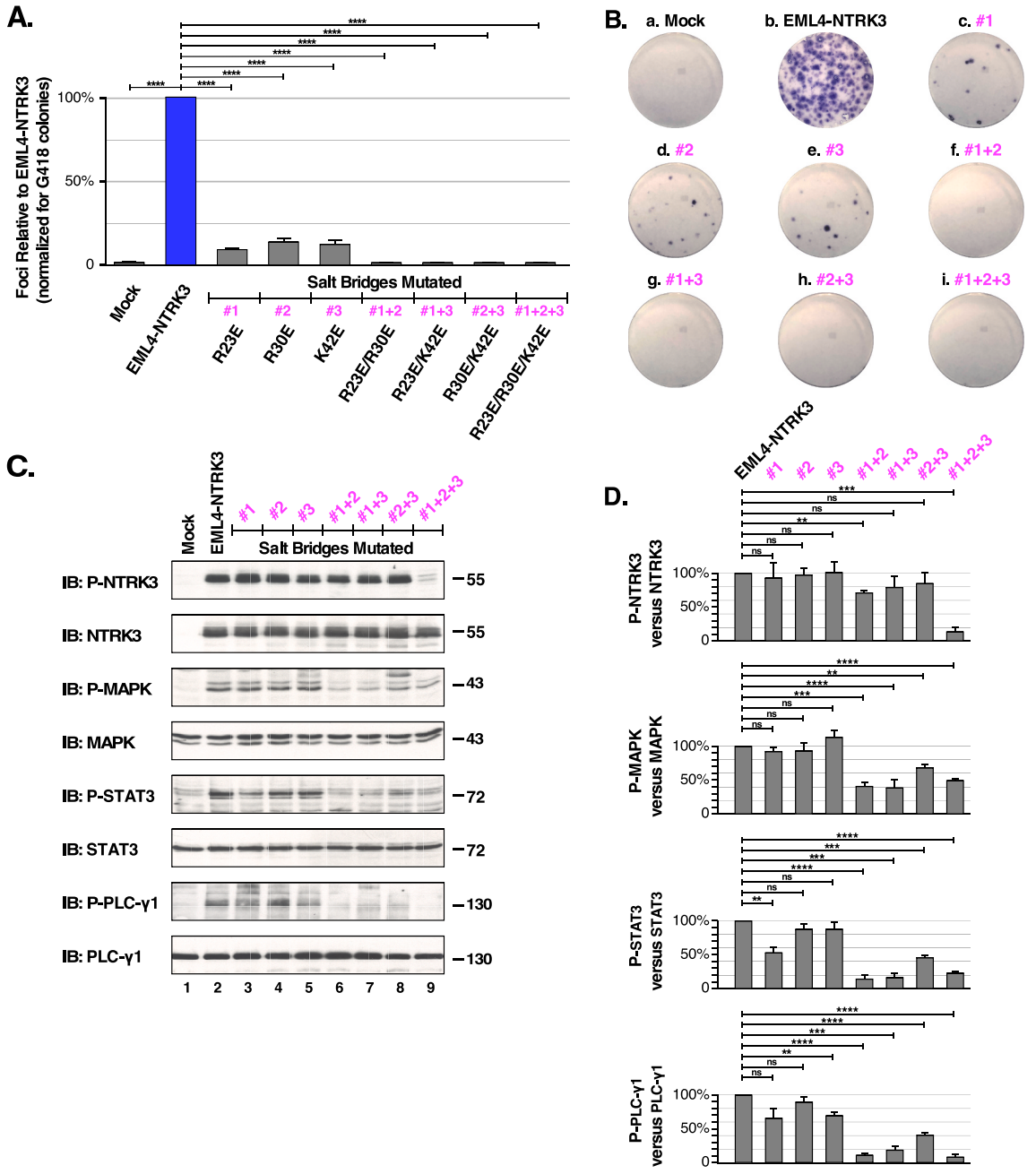


**Fig. 3. Abrogation of biological activity and downstream activation by salt bridge mutations. (A)** The graph shows the results from NIH3T3 cell transformation assays. Foci were counted, normalized for transfection efficiency, and presented as a percentage of transformation in comparison with EML4-NTRK3 −/+ SEM. Assays were conducted a minimum of three times for each DNA construct. Results of two tailed paired t-tests are shown, where **** indicates significance at $P \leq 0.0001$. **(B)** Representative examples of NIH3T3 plates demonstrate transformation by the salt-bridge mutants of EML4-NTRK3, in the same order as in (A). Plates were fixed with methanol and stained using Giemsa. **(C)** Lysates of HEK293T cells expressing EML4-NTRK3 and the salt bridge mutants were immunoblotted for phospho-NTRK3 (top panel), phospho-MAPK (3rd panel), phospho-STAT3 (5th panel) and phospho-PLCγ (7th panel). Membranes were stripped and reprobed for total protein expression NTRK3 (2nd panel), MAPK (4th panel), STAT3 (6th panel) and PLCγ (8th panel). Supplementary data is included in the file Supplementary-Figure3C.pdf **(D)** Three independent replicates of immunoblots, including those presented in (C), were quantitated using ImageJ and then used to determine changes in P-NTRK3, P-MAPK, P-STAT3, and P-PLCγ1, after normalization with respect to total NTRK3, MAPK, STAT3, and PLCγ1. The P values of two-tailed paired t tests are presented for wild-type EML4-NTRK3 versus each of the single, double, and triple salt bridge mutants. Statistical significance is indicated: ns = not significant; * = $P \leq 0.05$; ** = $P \leq 0.01$; *** = $P \leq 0.001$; **** = $P \leq 0.0001$.

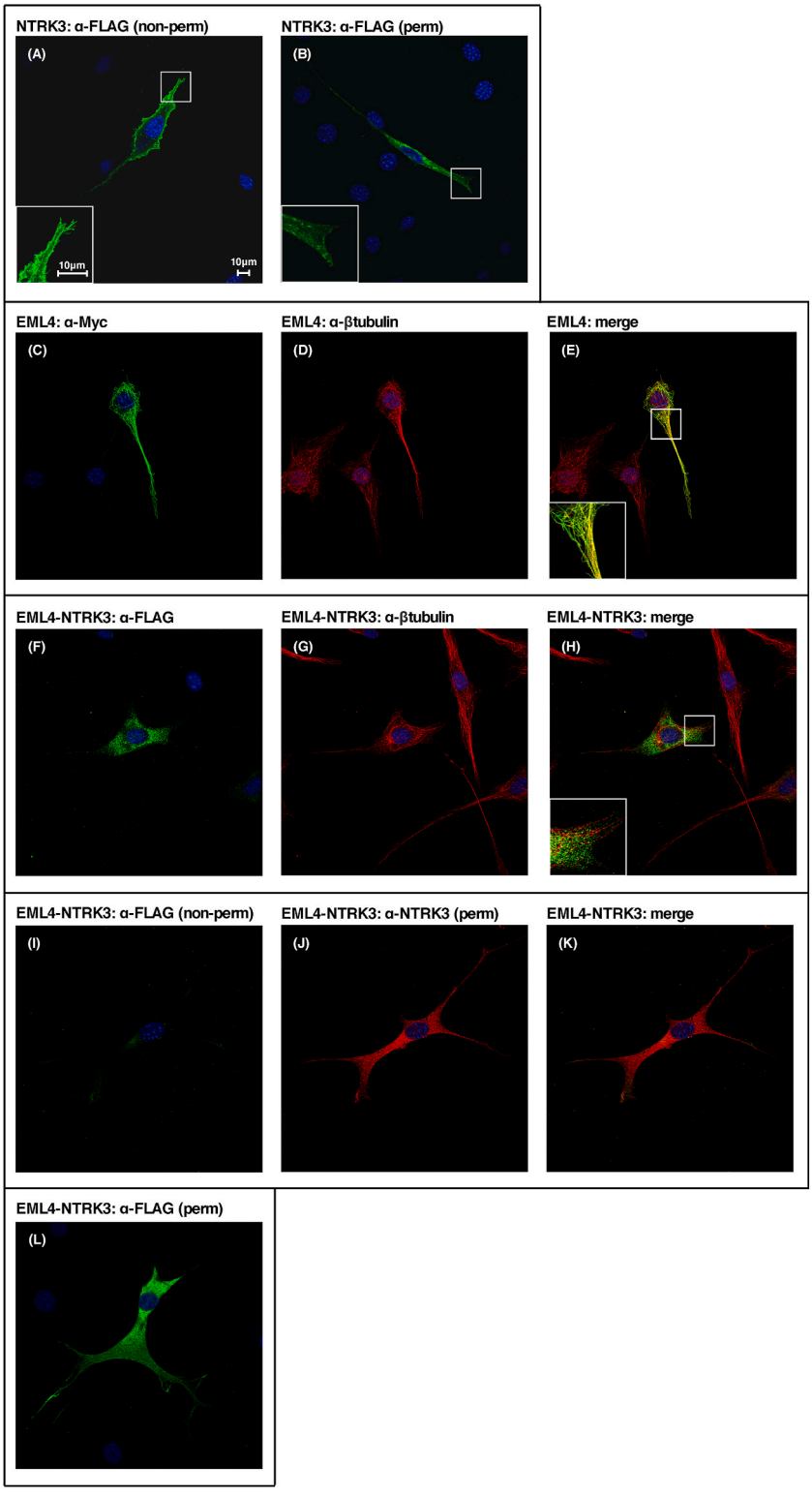


(caption on next page)

**Fig. 4. Subcellular localization of EML4-NTRK3.** A Leica SP8 inverted confocal microscope was employed to visualize the subcellular localization of Flag-NTRK3, Flag-EML4-NTRK3, and EML4-Myc proteins expressed in NIH3T3 cells. **(A,B)** Membrane localization of Flag-NTRK3 is shown in non-permeabilized cells in (A) and permeabilized cells in (B) using Flag antisera. The Flag tag was appended at the N-terminus of NTRK3, just after the signal cleavage site. **(C,D,E)** EML4-Myc was detected using Myc antisera in (C), while β-tubulin is seen in (D) and colocalizes with EML4-Myc in (E). **(F,G,H)** Flag-EML4-NTRK3 localization is visualized in the cytoplasm with Flag antisera (F), and β-tubulin is visualized for the same cell in (G); the signals for Flag-EML4-NTRK3 and β-tubulin do not colocalize as seen in (H). **(I,J,K)** No signal is detected for Flag-EML4-NTRK3 in a non-permeabilized cell in (I), but is visualized in the cytoplasm of the same cell after permeabilization with NTRK3 antisera (J). **(L)** As a control for the Flag antiserum used in (I), permeabilized cells expressing Flag-EML4-NTRK3 were stained with Flag antiserum as used in (I). The calibration bar shown in Panel A, in both the main image and the enlarged inset, represents 10 μm. All images are shown at the same magnification, and the insets shown are enlarged 250 % from the main image.

### *3.5. EML4 coiled-coil mimetic interaction with EML4-NTRK3 is dependent on electrostatic salt bridge interactions*

Given that the salt bridge residues are essential for the multimerization of EML4-NTRK3, we next designed an EML4 coiled-coil mimetic that can potentially abrogate the activity of EML4-NTRK3. The EML4 coiled-coil mimetic (cc-EML4) was created by isolating the Flag-tagged EML4 coiled-coil domain from EML4-NTRK3 (Fig. 5B). During the trimerization event of EML4-NTRK3, three copies of the fusion protein are brought together by the coiled-coil domain of EML4 to activate the NTRK3 kinase. Thus, we hypothesized that ccEML4 can replace one or more copies of the EML4-NTRK3 trimeric complex and interact with the remaining copies of the fusion protein.

HEK293T cells were co-transfected with either EML4-NTRK3 or EML4(R23E/R30E/K42E)-NTRK3, with or without Flag-tagged cc-EML4. Lysates were immunoprecipitated with anti-NTRK3 antiserum and immunoblotted to detect associated cc-EML4 (Fig. 5C, top panel). This experiment revealed that ccEML4 interacted with EML4-NTRK3 (lane 4), but not with EML4(R23E/R30E/K42E)-NTRK3 (lane 6). These data demonstrate that successful hetero-multimerization of EML4-NTRK3 requires the salt bridge interactions within the EML4 coiled-coil domain, and that cc-EML4 can hetero-multimerize with the EML4-NTRK3 fusion protein. The ability of a cc-EML4 mimetic to integrate into the EML4-NTRK3 trimeric complex demonstrates that the process of hetero-multimerization represents a potential therapeutic target.

## 4. Discussion

Mis-regulated tyrosine kinases represent a key target for personalized medicine and, through the characterization of tyrosine kinase fusion proteins, more therapeutic targets can be identified to overcome the resistance resulting from tyrosine kinase inhibitor treatments. Neurotrophic receptor tyrosine kinase 3 (NTRK3) is essential in regulating neuronal survival and fusion with an N-terminal partner gene such as ETV6-NTRK3 has been identified in various tumor types including IFS and glioma [11]. First discovered in 2015 in a case of IFS [4], the fusion protein EML4-NTRK3, comprised of the coiled-coil domain of EML4 and the tyrosine kinase domain of NTRK3, has also been found in several cases of IFS, Mammary Analog Secretory Carcinoma, Congenital Mesoblastic Nephroma, and Secretory Breast Carcinoma [9].

### *4.1. Characterization and downstream activation of EML4-NTRK3*

In this study, we further characterize EML4-NTRK3 biologically and biochemically. For biological assays, we utilized focus formation assays in the NIH3T3 murine fibroblast cell line, an assay that has served as an historically important biological readout for the identification and characterization of many different oncogenes [32,41,42]. This assay exploits the loss of contact inhibition which occurs in response to an oncogene, allowing cells to proliferate in response to the activation of oncogenic signaling pathways. From the focus formation assays in NIH3T3 cells, we demonstrate that the biological activity of EML4-NTRK3 relies on the kinase activity of NTRK3. EML4-NTRK3 possesses transforming activity, while the kinase-dead EML4-NTRK3(K572R) is unable to transform NIH3T3 cells (Fig. 1B and C). Through our analysis of downstream signaling, we show that EML4-NTRK3 activates ERK/MAPK, JAK/STAT3 and PKC/PLCγ pathways (Fig. 3C).

Previous studies showed that the N-terminus of EML4 can associate with the microtubules [10], which are associated with proliferation of cancer cells and metastasis [43]. Using indirect immunofluorescence, we verified the ability of EML4 to bind to microtubules, while EML4-NTRK3 localizes diffusely in the cytoplasm and does not localize to tubulin-like structures (Fig. 4), which demonstrates that the N-terminal coiled-coil domain is not sufficient for microtubule association.

### *4.2. Critical salt bridge interactions*

A previous study has shown the requirement of salt bridges for the transforming ability and downstream signaling pathways of the fusion protein, ETV6-NTRK3, which is also found in IFS [44]. The crystal structure of EML4 was solved, with the interhelical salt bridges identified [10]. However, whether the electrostatic interactions between the salt bridges are required to stabilize and activate the EML4-NTRK3 fusion had not been investigated. We found that disruption of all three salt bridges in the triple mutant, EML4 (R23E/R30E/K42E)-NTRK3, completely abrogates transforming activity of EML4-NTRK3 (Fig. 3A and B). The triple mutation almost completely eliminates activation of the NTRK3 receptor. Furthermore, activation of ERK/MAPK signaling is significantly diminished, while JAK/STAT3 and PKC/PLCγ signaling are reduced to an even greater extent (Fig. 3C and D). In general, each of the

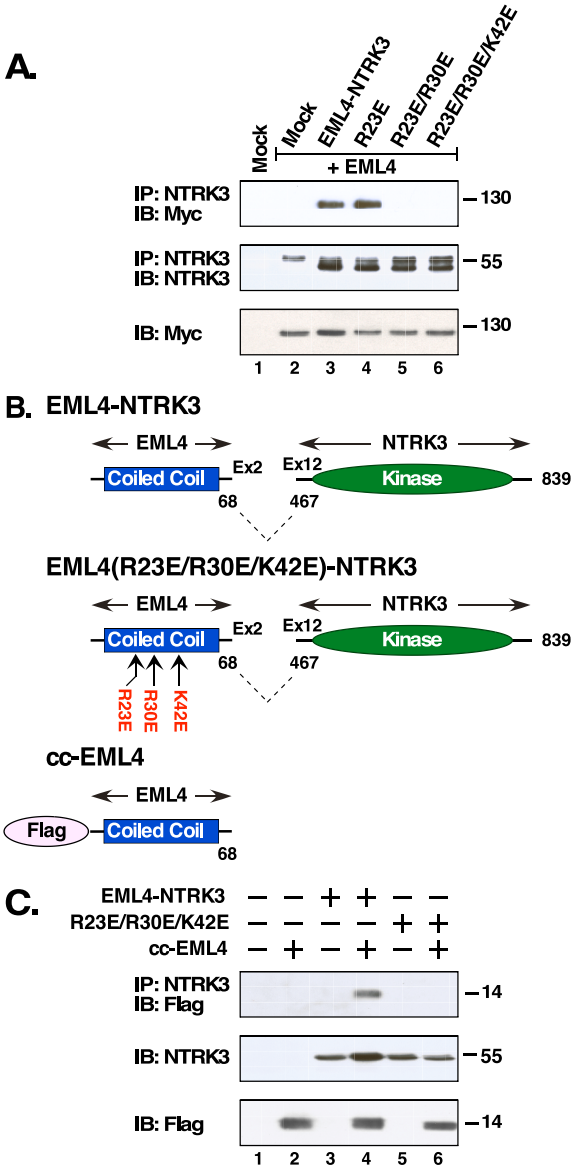


**Fig. 5. Abrogation of hetero-multimer formation by disruption of salt bridge interactions. (A)** HEK293T cells were co-transfected with EML4-NTRK3 or salt bridge mutants (R23E, R23E/R30E, and R23E/R30E/K42E) and EML4-Myc. Lysates were immunoprecipitated with NTRK3 antisera and immunoblotted with anti-Myc (top panel). The membrane was reprobed for the EML4-NTRK3 fusion proteins (middle panel, lower bands). Expression of EML4-Myc in total lysate is shown (lower panel). Supplementary data is included in the file Supplementary-Figure5A.pdf **(B)** Schematic of EML4-NTRK3, EML4(R23E/R30E/K42E)-NTRK3, and cc-EML4, which contains only the coiled-coil domain of EML4 and is Flag-tagged at the N-terminus. **(C)** cc-EML4 was co-transfected into HEK293T cells with either EML4-NTRK3 or EML4(R23E/R30E/K42E)-NTRK3. Cell lysates were immunoprecipitated using antibodies against NTRK3 and immunoblotted for the Flag-tagged cc-EML4. Cell lysates were also immunoblotted with NTRK3 antisera to detect EML4-NTRK3 and EML4(R23E/R30E/K42E)-NTRK3 (middle panel), and with Flag antisera to detect Flag-tagged cc-EML4 (bottom panel).

double salt bridge mutations results in greater loss of biological activity and signaling activity than each of the single salt bridge mutations. Interestingly, receptor activation as measured by activation loop phosphorylation diminishes significantly only in response to the triple mutation, suggesting that activation loop phosphorylation by itself is insufficient for downstream effects. Also, MAPK activation remains largely unaffected by single salt bridge mutations, although there is a clear reduction in response to double and triple mutations. At present, we cannot rule out the possibility that disruption of the salt bridges results in misfolding of the coiled coil as opposed to a loss of oligomerization with retention of α-helical structure. While we favor the latter, direct demonstration would be a valuable future experimental goal.

In the multimerization assay, disruption of all three salt bridges in the triple mutant also prevents the association of EML4-NTRK3 with EML4; this is also true for the double mutant EML4(R23E/R30E)-NTRK3. However, disrupting only one salt bridge, as in EML4

(R23E)-NTRK3, still allows hetero-multimerization (Fig. 5A). Taken together, these results indicate that the three salt bridges can cooperate to preserve the stability of the EML4 coiled-coil domain, multimerization ability and oncogenic activity of EML4-NTRK3.

The possibility of blocking salt bridge interactions as a therapeutic approach has recently been validated with the salt bridges found in Influenza A nucleoprotein. The Influenza A nucleoprotein undergoes trimerization which is stabilized by a highly conserved salt bridge between E339 and R416. Inhibitors were designed to block the interactions between those residues, preventing the nucleoprotein from trimerization. The inhibitors tested exhibit better potencies than commercially available neuraminidase inhibitors for H1N1 influenza virus strains [45].

### *4.3. Novel therapeutic targets for EML4-NTRK3 expressing cancers*

The treatment for IFS mostly involves surgical resection and TKI treatment. From the data presented, we identified two potential therapeutic targets for EML4-NTRK3 induced IFS based upon the N-terminus of EML4: first, disruption of electrostatic interactions between the salt bridge residues that stabilize EML4 coiled-coil domain and, second, the introduction of small molecule peptides that mimic the EML4 oligomerization domain.

A previous study has shown that monomerization of ALK fusion proteins, facilitated by EML4 coiled-coil peptides, could be a therapeutic approach for non-small cell lung cancer [46]. However, whether the same therapeutic strategy can be used for NTRK-rearranged fusion proteins has not been previously determined. Our data demonstrate that when both cc-EML4 and EML4-NTRK3 are present in cells, cc-EML4 can integrate into the EML4-NTRK3 trimeric complex and hetero-multimerize with the fusion protein. Moreover, this association is dependent upon the salt bridge interactions in the EML4 coiled-coil domain (Fig. 5C). This association can potentially reduce the NTRK3 kinase activity and the oncogenic activity of EML4-NTRK3. Thus, the process of multimerization of EML4-NTRK3 by the coiled-coil domain has the potential to serve as an additional therapeutic target in EML4-NTRK3 positive Infantile Fibrosarcoma patients.

## 5. Conclusions

Taken together, we assessed the importance of salt bridge interactions and multimerization within the coiled-coil domain of EML4 in the biological activity of the fusion EML4-NTRK3. We demonstrate that disruption of salt bridge interactions leads to inhibition of multimerization and abrogation of downstream signaling cascades, providing a novel target for TKI resistant EML4-NTRK3-positive sarcomas.

## Funding statement

DJD gratefully acknowledges generous philanthropic support from the UC San Diego Foundation.

## Data availability statement

All materials and data described will be made available to members of the scientific community upon request.

## Ethics approval

This work does not involve the use of human or animal subjects; therefore, approval was not required from the UCSD Institutional Review Board or from the UCSD Institutional Animal Care and Use Committee.

## CRediT authorship contribution statement

**Zian Jiang:** Writing – review & editing, Writing – original draft, Validation, Methodology, Investigation, Conceptualization. **April N. Meyer:** Writing – review & editing, Writing – original draft, Validation, Supervision, Methodology, Investigation. **Wei Yang:** Writing – review & editing, Validation, Methodology, Investigation. **Daniel J. Donoghue:** Writing – review & editing, Writing – original draft, Validation, Supervision, Resources, Project administration, Methodology, Investigation, Funding acquisition, Data curation, Conceptualization.

## Declaration of competing interest

The authors declare that they have no known competing financial interests or personal relationships that could have appeared to influence the work reported in this paper.

## Acknowledgements

We thank all current and past lab members, particularly Nicole Peiris and Megha Aepala, for valuable suggestions to the experimental design and final manuscript. The UC San Diego Neuroscience Microscope Facility was supported by NINDS P30 NS047101.

## Appendix A. Supplementary data

Supplementary data to this article can be found online at https://doi.org/10.1016/j.heliyon.2024.e36278.

## References


[1] D. Orbach, A. Rey, G. Cecchetto, O. Oberlin, M. Casanova, E. Thebaud, et al., Infantile fibrosarcoma: management based on the European experience, J. Clin. Oncol. 28 (2010) 318–323.
[2] L. Parida, I. Fernandez-Pineda, J.K. Uffman, A.M. Davidoff, M.J. Krasin, A. Pappo, et al., Clinical management of infantile fibrosarcoma: a retrospective single-institution review, Pediatr. Surg. Int. 29 (2013) 703–708.
[3] E.B. Chung, F.M. Enzinger, Infantile fibrosarcoma, Cancer 38 (1976) 729–739.
[4] S. Tannenbaum-Dvir, J.L. Glade Bender, A.J. Church, K.A. Janeway, M.H. Harris, M.M. Mansukhani, et al., Characterization of a novel fusion gene EML4-NTRK3 in a case of recurrent congenital fibrosarcoma, Cold Spring Harb Mol Case Stud 1 (2015) a000471.
[5] M.R. Aepala, M.N. Peiris, Z. Jiang, W. Yang, A.N. Meyer, D.J. Donoghue, Nefarious NTRK oncogenic fusions in pediatric sarcomas: too many to Trk, Cytokine Growth Factor Rev. 68 (2022) 93–106.
[6] J.M. Bourgeois, S.R. Knezevich, J.A. Mathers, P.H. Sorensen, Molecular detection of the ETV6-NTRK3 gene fusion differentiates congenital fibrosarcoma from other childhood spindle cell tumors, Am. J. Surg. Pathol. 24 (2000) 937–946.
[7] S.R. Knezevich, D.E. McFadden, W. Tao, J.F. Lim, P.H. Sorensen, A novel ETV6-NTRK3 gene fusion in congenital fibrosarcoma, Nat. Genet. 18 (1998) 184–187.
[8] C. Lazzari, L. Pecciarini, C. Doglioni, F. Pedica, A.M.S. Gajate, A. Bulotta, et al., Case report: EML4::NTRK3 gene fusion in a patient with metastatic lung adenocarcinoma successfully treated with entrectinib, Front. Oncol. 12 (2022) 1038774.
[9] A.J. Church, M.L. Calicchio, V. Nardi, A. Skalova, A. Pinto, D.A. Dillon, et al., Recurrent EML4-NTRK3 fusions in infantile fibrosarcoma and congenital mesoblastic nephroma suggest a revised testing strategy, Mod. Pathol. 31 (2018) 463–473.
[10] M.W. Richards, L. O'Regan, D. Roth, J.M. Montgomery, A. Straube, A.M. Fry, et al., Microtubule association of EML proteins and the EML4-ALK variant 3 oncoprotein require an N-terminal trimerization domain, Biochem. J. 467 (2015) 529–536.
[11] W. Jin, Roles of TrkC signaling in the regulation of tumorigenicity and metastasis of cancer, Cancers 12 (2020).
[12] C.A. Manea, D.C. Badiu, I.C. Ploscaru, A. Zgura, X. Bacinschi, C.G. Smarandache, et al., A review of NTRK fusions in cancer, Ann Med Surg (Lond). 79 (2022) 103893.
[13] M.S. Kim, J. Jeong, J. Seo, H.S. Kim, S.J. Kim, W. Jin, Dysregulated JAK2 expression by TrkC promotes metastasis potential, and EMT program of metastatic breast cancer, Sci. Rep. 6 (2016) 33899.
[14] S. Lawn, N. Krishna, A. Pisklakova, X. Qu, D.A. Fenstermacher, M. Fournier, et al., Neurotrophin signaling via TrkB and TrkC receptors promotes the growth of brain tumor-initiating cells, J. Biol. Chem. 290 (2015) 3814–3824.
[15] L.M. McGregor, B.K. McCune, J.R. Graff, P.R. McDowell, K.E. Romans, G.D. Yancopoulos, et al., Roles of trk family neurotrophin receptors in medullary thyroid carcinoma development and progression, Proc Natl Acad Sci U S A. 96 (1999) 4540–4545.
[16] D.A. Siegel, J. King, E. Tai, N. Buchanan, U.A. Ajani, J. Li, Cancer incidence rates and trends among children and adolescents in the United States, 2001-2009, Pediatrics 134 (2014) e945–e955.
[17] N. Ichaso, R.E. Rodriguez, D. Martin-Zanca, R. Gonzalez-Sarmiento, Genomic characterization of the human trkC gene, Oncogene 17 (1998) 1871–1875.
[18] A.J. Peterson, M. Kyba, D. Bornemann, K. Morgan, H.W. Brock, J. Simon, A domain shared by the Polycomb group proteins Scm and ph mediates heterotypic and homotypic interactions, Mol. Cell Biol. 17 (1997) 6683–6692.
[19] C.D. Thanos, K.E. Goodwill, J.U. Bowie, Oligomeric structure of the human EphB2 receptor SAM domain, Science 283 (1999) 833–836.
[20] E. Palmerini, G. Frega, M. Gambarotti, T. Frisoni, M. Cesari, A. Bazzocchi, et al., NTRK rearranged sarcoma of the bone. Role for larotrectinib in the neoadjuvant setting of an ultra-rare tumor: a case report, Front. Oncol. 13 (2023) 1252359.
[21] S. Wu, Y. Liu, K. Li, Z. Liang, X. Zeng, Molecular and cytogenetic features of NTRK fusions enriched in BRAF and RET double-negative papillary thyroid cancer, J. Mol. Diagn. 25 (2023) 569–582.
[22] S. Wu, Y. Liu, X. Shi, W. Zhou, X. Zeng, Elaboration of NTRK-rearranged colorectal cancer: integration of immunoreactivity pattern, cytogenetic identity, and rearrangement variant, Dig. Liver Dis. 55 (2023) 1757–1764.
[23] X. Dang, T. Xiang, C. Zhao, H. Tang, P. Cui, EML4-NTRK3 fusion cervical sarcoma: a case report and literature review, Front. Med. 9 (2022) 832376.
[24] F. Pasleau, M.J. Tocci, F. Leung, J.J. Kopchick, Growth hormone gene expression in eukaryotic cells directed by the Rous sarcoma virus long terminal repeat or cytomegalovirus immediate-early promoter, Gene 38 (1985) 227–232.
[25] A.D. Miller, G.J. Rosman, Improved retroviral vectors for gene transfer and expression, Biotechniques 7 (980–2) (1989) 9–90, 4-6.
[26] H. Liu, J.H. Naismith, An efficient one-step site-directed deletion, insertion, single and multiple-site plasmid mutagenesis protocol, BMC Biotechnol. 8 (2008) 91.
[27] K.N. Nelson, A.N. Meyer, C.G. Wang, D.J. Donoghue, Oncogenic driver FGFR3-TACC3 is dependent on membrane trafficking and ERK signaling, Oncotarget 9 (2018) 34306–34319.
[28] K.N. Nelson, A.N. Meyer, A. Siari, A.R. Campos, K. Motamedchaboki, D.J. Donoghue, Oncogenic gene fusion FGFR3-TACC3 is regulated by tyrosine phosphorylation, Mol. Cancer Res. 14 (2016) 458–469.
[29] B.A. Weaver, Z.Q. Bonday, F.R. Putkey, G.J. Kops, A.D. Silk, D.W. Cleveland, Centromere-associated protein-E is essential for the mammalian mitotic checkpoint to prevent aneuploidy due to single chromosome loss, J. Cell Biol. 162 (2003) 551–563.
[30] P. Bomont, P. Maddox, J.V. Shah, A.B. Desai, D.W. Cleveland, Unstable microtubule capture at kinetochores depleted of the centromere-associated protein CENP-F, EMBO J. 24 (2005) 3927–3939.
[31] M.N. Peiris, A.N. Meyer, K.N. Nelson, E.W. Bisom-Rapp, D.J. Donoghue, Oncogenic fusion protein BCR-FGFR1 requires BCR-mediated oligomerization and chaperonin Hsp90 for activation, Haematologica 105 (2020) 1262–1273.
[32] C. Shih, B.Z. Shilo, M.P. Goldfarb, A. Dannenberg, R.A. Weinberg, Passage of phenotypes of chemically transformed cells via transfection of DNA and chromatin, Proc Natl Acad Sci U S A. 76 (1979) 5714–5718.
[33] R.A. Padua, G. Carter, D. Hughes, J. Gow, C. Farr, D. Oscier, et al., RAS mutations in myelodysplasia detected by amplification, oligonucleotide hybridization, and transformation, Leukemia 2 (1988) 503–510.
[34] S. Bafna, A.P. Singh, N. Moniaux, J.D. Eudy, J.L. Meza, S.K. Batra, MUC4, a multifunctional transmembrane glycoprotein, induces oncogenic transformation of NIH3T3 mouse fibroblast cells, Cancer Res. 68 (2008) 9231–9238.
[35] M. Sun, G. Wang, J.E. Paciga, R.I. Feldman, Z.Q. Yuan, X.L. Ma, et al., AKT1/PKBalpha kinase is frequently elevated in human cancers and its constitutive activation is required for oncogenic transformation in NIH3T3 cells, Am. J. Pathol. 159 (2001) 431–437.
[36] J.P. Schneider, A. Lombardi, W.F. DeGrado, Analysis and design of three-stranded coiled coils and three-helix bundles, Folding Des. 3 (1998) R29–R40.
[37] E. Cocco, M. Scaltriti, A. Drilon, NTRK fusion-positive cancers and TRK inhibitor therapy, Nat. Rev. Clin. Oncol. 15 (2018) 731–747.
[38] L.F. Reichardt, Neurotrophin-regulated signalling pathways, Philos. Trans. R. Soc. Lond. B Biol. Sci. 361 (2006) 1545–1564.
[39] L.M. Weiss, V.A. Funari, NTRK fusions and Trk proteins: what are they and how to test for them, Hum. Pathol. 112 (2021) 59–69.
[40] R. Adib, J.M. Montgomery, J. Atherton, L. O'Regan, M.W. Richards, K.R. Straatman, et al., Mitotic phosphorylation by NEK6 and NEK7 reduces the microtubule affinity of EML4 to promote chromosome congression, Sci. Signal. 12 (2019).

[41] P. Andersson, M.P. Goldfarb, R.A. Weinberg, A defined subgenomic fragment of in vitro synthesized Moloney sarcoma virus DNA can induce cell transformation upon transfection, Cell. 16 (1979) 63–75.
[42] N.G. Copeland, A.D. Zelenetz, G.M. Cooper, Transformation of NIH/3T3 mouse cells by DNA of Rous sarcoma virus, Cell 17 (1979) 993–1002.
[43] A.L. Parker, M. Kavallaris, J.A. McCarroll, Microtubules and their role in cellular stress in cancer, Front. Oncol. 4 (2014) 153.
[44] N. Cetinbas, H. Huang-Hobbs, C. Tognon, G. Leprivier, J. An, S. McKinney, et al., Mutation of the salt bridge-forming residues in the ETV6-SAM domain interface blocks ETV6-NTRK3-induced cellular transformation, J. Biol. Chem. 288 (2013) 27940–27950.
[45] J.L. Woodring, S.H. Lu, L. Krasnova, S.C. Wang, J.B. Chen, C.C. Chou, et al., Disrupting the conserved salt bridge in the trimerization of influenza A nucleoprotein, J. Med. Chem. 63 (2020) 205–215.
[46] N. Hirai, T. Sasaki, S. Okumura, Y. Minami, S. Chiba, Y. Ohsaki, Monomerization of ALK fusion proteins as a therapeutic strategy in ALK-rearranged non-small cell lung cancers, Front. Oncol. 10 (2020) 419.